Korean J. Chem. Eng., 37(12), 2351-2358 (2020)
DOI: 10.1007/s11814-020-0664-5

pISSN: 0256-1115
eISSN: 1975-7220

Synthesis and characterization of hydroxyethyl cellulose (HEC)-TiO_2-based polyurethane bionanocomposites

Muhammad Fiayaz*, Khalid Mahmood Zia*,†, Muhammad Asif Javaid, Saima Rehman***, Shahzad Ali Shahid Chatha***, and Mohammad Zuber***

*Department of Applied Chemistry, Government College University, Faisalabad 38030-Pakistan
**Department of Chemistry, University of Agriculture, Faisalabad 38040-Pakistan
***Department of Chemistry, Government College University, Faisalabad 38030-Pakistan
(*Received 17 June 2020 • Revised 9 August 2020 • Accepted 17 August 2020*)

Abstract−A novel green series of hydroxyethyl cellulose (HEC) based polyurethane (PUs) prepolymersblended with TiO_2 nanoparticles were synthesized by reaction of Isophorone diisocyanate (IPDI), hydroxyl-terminated polybutadiene (HTPB), and hydroxyethyl cellulose (HEC). The chain was further extended with 1,4-butanediol (BDO) to get final HEC based polyurethane bio nanocomposites (FPUNC). A mixture of HEC based polymer and TiO_2 nanoparticles was formed in solution polymerization, in which the TiO_2 nanoparticles dispersed depending on interaction of TiO_2 nanoparticles with polymer chains. The molecular structure of the synthesized PU bionanocomposites was confirmed by FTIR. A series of FPUNCs was prepared by varying the percent composition of the TiO_2 nanoparticles into the PU matrix. The morphology of the bionanocomposites was carried out by X-ray diffraction (XRD) studies and scanning electron microscopy (SEM). SEM images verified the good dispersion of TiO_2 nanoparticles into PU matrix. The thermal stability of the synthesized FPUNCs was done by thermal gravimetric analysis (TGA), and the FPUNC12 with 5% contents of TiO_2 nanoparticles showed better thermal stability. The resultant HEC-TiO_2 based FPUNCs material have promising bio-degradable and bio functional materials with good thermal properties and have potential applications in the field of biomaterials.

Keywords: Hydroxyethylcellulose, Polyurethane, Biomaterials, TiO_2 Nanoparticles, FTIR, SEM, XRD, TGA

INTRODUCTION

Synthetic polymers have been used in a number of applications, such as food packaging materials, plastics, automotive industry, electronics, clothing and protective coatings. Petroleum derivatives have been their raw materials so far. Increasing complaints of environmental contamination, toxicity, non-biodegradability and price dependence on crude oil rates have made researchers think of their alternatives [1-3]. Polysaccharide based polymeric materials have received great attention in recent years, mainly because of their easy availability, economical and biodegradability concerns. Cellulose, chitin, chitosan, starch, pectin and other seed oil based polymers and nanocomposites have been prepared with enhanced features. The nanometer size of the filler nanoparticles and huge surface area increases the interface between both the phases. The polymer and filler interfacial interaction is enhanced, resulting in improved material properties [4]. The polymers and nanocomposites thus prepared have shown good barrier qualities, better thermal and mechanical properties and industrial impact. Most importantly, being originated from plant sources they are cheap, biodegradable, environment friendly and also have many medical applications. The field of biobased polymers and their nanocomposites is creating many exciting new materials with novel properties. Cellulose and its derivatives have been explored as a probable source for advanced materials, especially in biomedical and industrial engineering [2,5-7]. Cellulose whiskers and nanofibrils have been used in a number of studies with the features of biodegradability along with additional properties. Hydroxyethyl cellulose (HEC), an important polymer from the cellulose family, possesses excellent biodegradable, film forming and biocompatible properties with great potential in the fields of biomedical, dyeing, paper making, coatings, fibers, pesticides and medicine [5,8,9].

Polyurethanes are a unique class of polymers with a long list of versatile applications because of a wide range of physical and mechanical properties. They can be tailor-made with the possibility of varied range of synthetic options [10]. Polyurethanes provide an extensive range of matrix for the synthesis of tunable nanocomposites with good thermal, mechanical properties and applications [11] Polyurethane elastomers (PUEs) are a distinctive class of polymers due to their biodegradable and biocompatible properties [12,13]. The functionalization of polyurethanes has also been reported through the different polysaccharides [14]. Cellulose, starch, pectin, chitin, chitosan, and alginates functionalized polyurethanes have been reported in the literature [7,8,17-19]. Titanium dioxide (TiO_2) is inert, nontoxic and is widely used in the synthesis of biodegradable films with antimicrobial and anti-radiation properties. The polymer nanocomposites with TiO_2 have been prepared with excellent mechanical and anti-bacterial properties [3].

†To whom correspondence should be addressed.
E-mail: ziakmpkpolym@yahoo.com

In the field of advanced coatings, many nanoparticles like nanoclay, ZnO, SiO_2, CNT and TiO_2 have been combined with PU matrix. Researchers have reported a graft copolymer of water-soluble 2-hydroxyethyl cellulose (2-HEC) and lactic acid (LA) [13]. Sepiolite/PU composites with nanostructure have been reported [4]. Sunflower-oil based polyurethane-TiO_2 nanocomposite coatings have been prepared [1]. Surface characteristics of starch, cellulose, and triolein injected polyurethane have been studied. Whey protein-based bionanocomposite films with cellulose nanofibers and TiO_2 nanoparticles have been synthesized [3].

Evaluation of bionanocomposites, polystyrene/hydrophobic TiO_2 nanobelts as packaging material [20,21] and preparation and utilization of polystyrene nanocomposites based on TiO_2 nanowires [22] have the interest of many researchers. Morphological studies of polyaniline nanocomposite based mesostructured TiO_2 nanowires as conductive packaging materials and TiO_2 nanowires and TiO_2 nanowires doped Ag-PVP nanocomposites for antimicrobial and self-cleaning cotton textile have also been extensively studied [23,24]. Mechanical properties of PU were improved with the involvement of low fractions of cellulose nanocrystals (CNC) and bio-based polyols [25]. The synergistic conduct of starch nanoparticles and cellulose particles has been studied in the synthesis of water-based polyurethane [26]. HEC/polyaniline based nanocomposite cryogels have been prepared having potential applications in tissue engineering [27].

Keeping in view the versatile properties and application of the HEC, TiO_2 nanoparticles and polyurethane elastomers, the current study synthesized novel HEC based polyurethane bionanocomposites having TiO_2 which, to the best of our knowledge, has not been reported yet. Their chemical, morphological and thermal properties have been investigated using Fourier transform infrared analysis (FT-IR), X-Ray diffraction studies (XRD), scanning electron microscopy (SEM) and thermogravimetric analysis (TGA).

EXPERIMENTAL

1. Chemicals

Hydroxyethylcellulose (HEC), HTPB, IPDI, DMSO and BDO were acquired from Sigma-Aldrich Chemical Co (St. Louis, Missouri, United States). The TiO_2 nanoparticles (titanium (IV) oxide nanopowder, having crystal phase rutile with particle size 40 nm to >100 nm) were procured from Merck (Merck KGaA, Darmstadt, Germany). The BDO used was treated for exhaustion of gases at standard temperature that might otherwise interfere with isocyanate reactions. IPDI and rest of the chemicals were consumed without any treatment. All of the reagents used in this study were of analytical grade.

2. Preparation of HEC and TiO_2 Nanoparticle Based PU Prepolymer

The prepolymer was synthesized as reported in the literature. According to the established method, the polyurethane (PU) prepolymer was prepared by step-growth polymerization (two-step mechanism). In the first step, weighed amounts of TiO_2 nanoparticles and Hydroxyethylcellulose (HEC) were mixed in solvent (DMSO) separately and stirred till homogenization for 1 h each. Subsequently, the NCO terminated prepolymer was prepared by reacting diisocyanate (3 moles) and diol (1 mole). This was done by taking the homogenized TiO_2 nanoparticles, HEC solvent mixtures and the polyol HTPB in a four-necked retort flask. This reaction flask was equipped with an electric stirrer, N_2 environment, a reflux condenser and warming oil bath. The whole mixture was continuously stirred for 1 h with oil bath temperature set to 70 °C. The formation of prepolymer was finalized by addition of the diisocyanate IPDI into the above mixture with continuous stirring, keeping the temperature at 90 °C for another hour. The progress of prepolymer reaction was confirmed by obtaining its FTIR spectrum.

3. Preparation of HEC Based Polyurethane Bionanocomposites by Varying TiO_2 Nanoparticle Contents (FPUNC7-FPUNC13)

In the second step, the synthesized prepolymers were converted into final HEC based polyurethane bionanocomposites (FPUNCs) by the addition of a previously degassed alkane diol (chain extender). The 1,4-BDO was added into the reaction mixture at 85-90 °C under continuous stirring till uniformity in the final PU polymer was acquired. In this way, after optimizing the reaction conditions eight samples of FPUNCs were prepared by varying the content of TiO_2 nanoparticles and designated as FPU4 (0%) and FPUNC7-FPUNC13 having 0.5%, 1%, 2%, 3%, 4%, 5% and 8% TiO_2 nanoparticles by weight, respectively. The complete preparation designs are presented in Table 1.

The reaction mixture was observed closely for color homogeneity representing the complete dispersion of chain extender, hence the reaction was considered to be completed. The sticky polymer was cast down to the Teflon plate to get a uniform elastomeric film of 2-3 mm width. The prepared samples were treated under vacuum for 15 minutes to remove the solvent and any air bubbles therein prior to casting. Then the prepared bionanocomposite samples were cured at 100 °C for 24 hours in hot air oven. After curing the synthesized samples were kept at room temperature for a week before further analysis. The diagrammatic path for the preparation of HEC based polyurethane bionanocomposites varying TiO_2 contents is presented in Fig. 1.

4. Characterization

The molecular characterization of the prepared NCO-terminated HEC/TiO_2 nanoparticle based PU prepolymer and the final bion-

Table 1. Sample code designation and different formations of TiO_2 based polyurethane bionanocomposites

Sample code	HEC (moles)	HTPB (moles)	IPDI (moles)	BDO (moles)	TiO_2 %
FPU4	0.3	0.7	3.0	2.0	0.0
FPUNC7	0.3	0.7	3.0	2.0	0.5
FPUNC8	0.3	0.7	3.0	2.0	1.0
FPUNC9	0.3	0.7	3.0	2.0	2.0
FPUNC10	0.3	0.7	3.0	2.0	3.0
FPUNC11	0.3	0.7	3.0	2.0	4.0
FPUNC12	0.3	0.7	3.0	2.0	5.0
FPUNC13	0.3	0.7	3.0	2.0	8.0

FPU=Fiayaz polyurethane, HEC=2-Hydroxyethyl cellulose, HTPB=Hydroxyterminated polybutadiene, IPDI=Isophronediisocyanate, BDO=1,4-Butanediol, TiO_2=Titanium dioxide nanoparticles

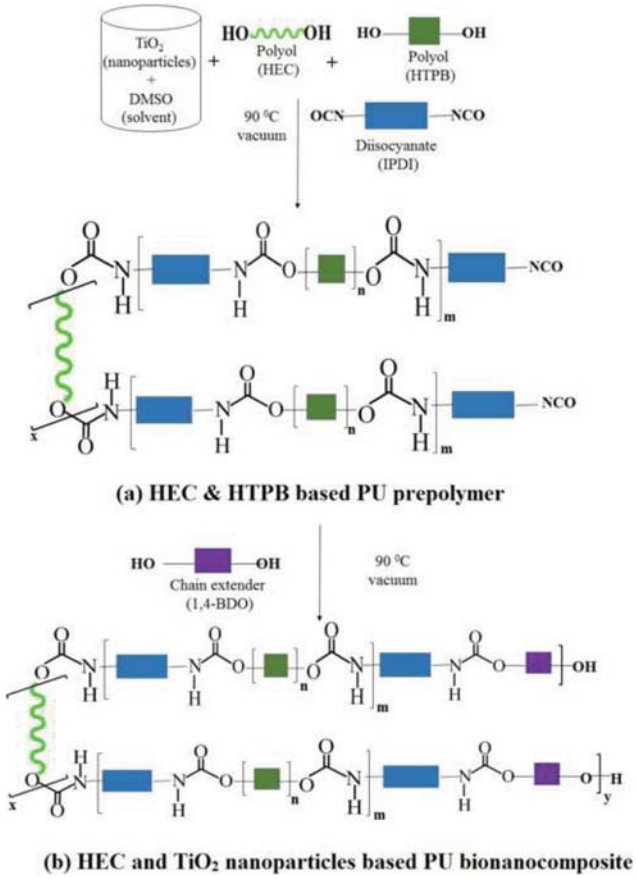

Fig. 1. Reaction scheme for synthesis of HEC based polyurethane bionanocomposites by varying TiO_2 nanoparticle content.

anocomposite PU films (FPUNC7-FPUNC13) was performed using FTIR spectroscopy. FTIR spectra were observed on a Bruker-IFS 48 Fourier transform infrared spectrophotometer (Ettlingen, Germany). These scans covered the infrared region 4,000 to 500 cm^{-1} and are presented in Figs. 2 and 3. The XRD diffractograms of HEC based polyurethane bionanocomposites were obtained from Siemens D-5000 X-ray diffractometer at 25 °C, with Cu K# ($= 15.4 nm, 40 kV and 30 mA) radiations and are presented in Fig. 4. The surface morphology of the prepared bionanocomposites was studied with the help of SEM model S-4800 instrument. The SEM images provided the details of surface of the prepared films at various magnifications obtained after treating them with gold presented in Fig. 5. The thermal degradation of prepared FPUNCs was studied with the help of thermal gravimetric analysis (TGA) instrument (model: SDT Q600 V20.9 Build 20, TA Instruments, USA). The sample weight loss related to a certain temperature was studied by thermographs presented in Fig. 6 to examine the thermal stability of FPUNCs.

5. X-ray Diffraction Studies

The calculation of % crystallinity based on the area under the curves to quantitatively compare crystallinity of TiO_2-PU samples and control PU sample is a more reliable method. The degree of crystallinity (%) of the prepared PU bionanocomposites can be estimated multiplying the ratio of the crystalline peak area to total peak area by 100:

$$\text{Degree of crystallinity (\%)} = \frac{\text{Area of crystallite phases}}{\text{Area under the all peaks}} \times 100 \quad (1)$$

The d-spacing of different samples was determined by Debye-Scherrer (powder) method using Bragg's relation:

$$n\lambda = 2d \sin\theta \quad (2)$$

In this study the crystallite size was calculated by using the Scherrer equation. The crystalline size of different formations of TiO_2 based polyurethane bionanocomposites was calculated by using the mathematical form of Scherrer's equation [28]:

$$D = \frac{k\lambda}{\beta\cos\theta} \quad (3)$$

where,

D=grain size of the material or crystalline size; k=constant or the factor of the dimension shape; λ=the wavelength of X-ray radiation; β=the intensity of the full width half maxima; θ=indicate the Bragg's angle

The average crystalline size of the five samples FPU4 (pure) and FPUNC8-9 and FPUNC 11 and 13 was calculated and data is presented and discussed. The steps involved are: (1) Calculate 2 theta value and FWHM from dominant peak only by using nonlinear fit Gaussian method, (2) Convert 2 theta degree into radians, (3) Convert FWHM into radians, (4) Put values in above Eq. (I) and calculate "D", i.e., crystalline size, (5) Calculate d-spacing by Bragg's Eq., (6) Use Origin Lab tool for analysis.

RESULTS AND DISCUSSION

1. Molecular Characterization

The suggested structure of monomers and the synthesized HEC/TiO_2 nanoparticle based polyurethane bionanocomposites were studied with FT-IR technique in the field range of 4,000-500 cm^{-1}. The FT-IR spectra of HTPB, IPDI and BDO were discussed in our previous study [29,30]. The FT-IR spectra of HEC having major peaks have also been deliberated [31]. The FT-IR spectra of NCO terminated prepolymer and final PU bionanocomposites are presented in Fig. 2.

In the FT-IR spectrum of the prepolymer, Fig. 2(a), the NH peak was observed at 3,364.38 cm^{-1}, which was the confirmation of formation of -NHCOO, i.e., the urethane linkage. The -CH_2 stretching vibrations were observed at 2,923.52 and 2,840.51 cm^{-1}. An isocyanate peak of low intensity was observed at 2,268.66 cm^{-1}. This peak could be attributed to the -NCO end groups present in the prepolymer. The peaks at 1,703.29 cm^{-1} and 1,541.02 cm^{-1} were attributed to C-O and NH bending, respectively. The completion of reaction was indicated by the disappearance of -OH peak along with the reduction in the intensity of 0NCO peak, which is in accordance with the reported literature [29].

In Fig. 2(b) the FTIR spectrum of FPUNC8 is presented having the following peaks: the NH group peak appeared at 3,354.24 cm^{-1}, CH_2 asymmetric and symmetric stretching peaks at 2,920.64 cm^{-1} and 2,843.93 cm^{-1}, respectively; C=O peak at 1,697.56 cm^{-1};

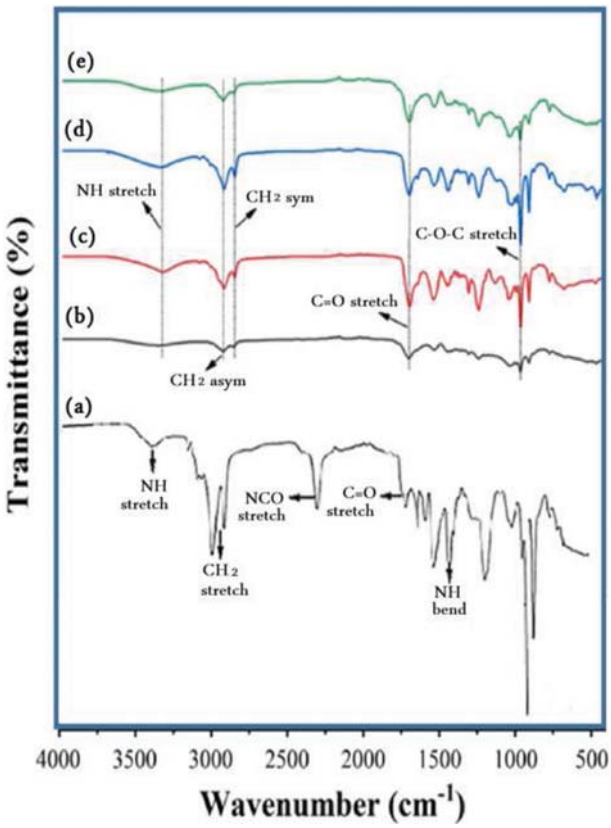

Fig. 2. FTIR spectra of HEC based PU prepolymer having TiO_2 nanoparticles and final PU bionanocomposites to confirm the proposed structure: (a) HEC & TiO_2 based PU prepolymer, (b) FPUNC8 (PU with 1% content of TiO_2 nanoparticles), (c) FPUNC9 (PU with 2% content of TiO_2 nanoparticles), (d) FPUNC11 (PU with 4% content of TiO_2 nanoparticles) and (e) (PU with 8% content of TiO_2 nanoparticles).

1,532.40 cm^{-1} for NH deformation and C-O-C widening peak appeared at 965.86 cm^{-1}.

In Fig. 2(c) FPUNC9 spectrum, the peak at 3,317.34 cm^{-1} is present due to NH groups; asymmetric and symmetric stretching of CH_2 at 2,915.43 cm^{-1} & 2,844.78 cm^{-1}, respectively; 1,537.47 cm^{-1} NH deformation; 1,694.03 cm^{-1} carbonyl group peak; 964.20 cm^{-1} C-O-C peak is present.

In Fig. 2(d) FPUNC11 spectrum, the peak at 3,335.39 cm^{-1} is due to NH group; CH_2 asymmetric peak at 2,915.06 cm^{-1} and CH_2 symmetric peak at 2,844.24 cm^{-1}; carbonyl group peak present at 1,696.31 cm^{-1}; deformation of NH peaks at 1,534.46 cm^{-1}; C-O widening peak was present at 1,238.49 cm^{-1}.

In Fig. 2(e) spectrum of FPUNC13, the peak at 3,334.81 cm^{-1} is present due to NH group; CH_2 asymmetric peak is present at 2,919.95 cm^{-1}; carbonyl group peak present at 1,695.81 cm^{-1}; deformation of NH peaks at 1,532.16 cm^{-1}, 1,438.29 cm^{-1}; C-O widening peak was present at 1,239.31 cm^{-1}.

Analysis of FT-IR in Fig. 2(a)-(e) shows the absence of -NCO peak and the appearance of wide peak of -NH pertaining to the reaction completion. FT-IR peaks with values between 3,300-3,350 cm^{-1} validate the existence of -NH stretching [32]. The observed peaks in the spectra in Fig. 2 (FPUNC8, FPUNC9, FPUNC11 and FPUNC13) imply the completion of reaction and predesigned HEC based polyurethane bionanocomposite varying TiO_2 nanoparticles was formed.

For comparative study, Fig. 3 presents the merged FT-IR spectra of synthesized FPUNCs having different content of TiO_2 nanoparticles. All the relevant peaks are overlapped and imply that there is no variation in the chemistry of the prepared FPUNCs and have alike chemical structure. Phase separation in polyurethane nanocomposites has been reported due to interactions between N-H group, carbonyl oxygen and ether oxygen [28]. For comparison FTIR curves of samples without TiO_2 (FPU4) against TiO_2 containing composite samples (FPUNC7-FPUNC13) are presented in Fig. 3. In FTIR results comparing control PU (FPU4) and TiO_2-PU samples (FPUNC7-FPUNC13), it can be seen that there is variation in the sharpness and intensity of the peaks in FTIR spectra. Such variation in peak intensity and sharpness can be the result of different amount of samples taken for the FTIR analysis. The shift of peaks in the FTIR spectra can indicate the presence of second-

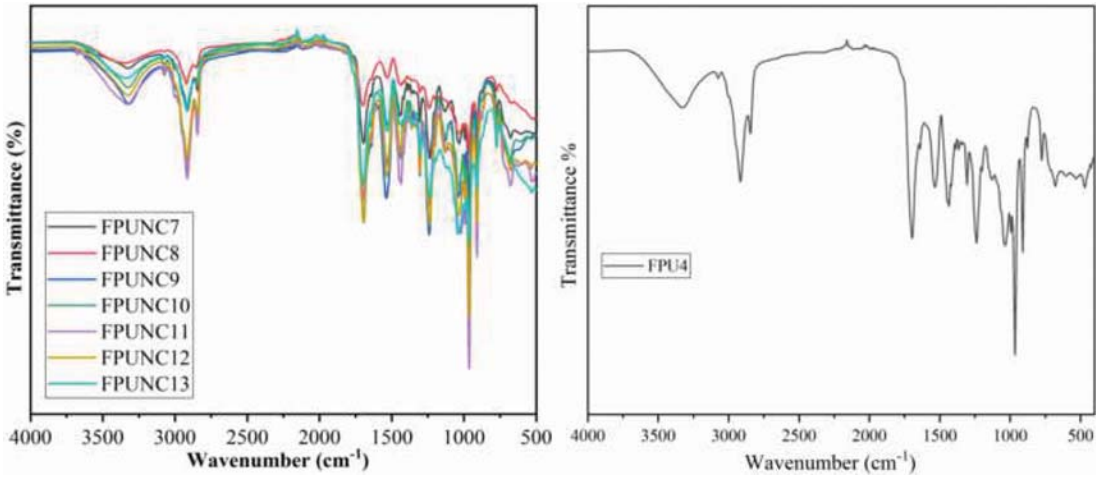

Fig. 3. FTIR spectra of HEC based PU bionanocomposites having TiO_2 nanoparticles FPUNC7-FPUNC13 and sample FPU4, pristine PU having zero content of TiO_2.

Table 2. Thermo-gravimetric analysis (TGA) data of HEC based PU bionanocomposites with TiO_2 nanoparticles

Sample code	TiO_2 wt (%)	$T_{-20\%}$ (°C)	$T_{-80\%}$ (°C)	$T_{max.}$ (°C)	Char residue (%)
FPU4	0.0	333	461	592	1.9
FPUNC7	0.5	330	452	584	1.0
FPUNC8	1.0	328	454	587	3.5
FPUNC9	2.0	307	457	587	4.6
FPUNC10	3.0	314	465	591	4.2
FPUNC11	4.0	315	459	585	5.3
FPUNC12	5.0	344	465	591	5.6
FPUNC13	8.0	325	458	589	6.4

ary interactions. There is no shift in the FTIR spectra (Figs. 2 and 3), which clearly supports the evidence regarding the absence of secondary interactions.

2. X-ray Diffraction Studies

The morphology of the prepared bionanocomposites was studied with XRD. The effect of incorporation of TiO_2 nanoparticles into the HEC based PUs was examined. The degree of crystallinity (%) of the prepared PU bionanocomposites was calculated based on the area under the curves to quantitatively compare crystallinity of TiO_2-PU samples and control PU sample, and results are reported in Table 3. The XRD patterns of the synthesized bionanocomposite samples are shown in Fig. 4. The size of sub-micrometer crystallites in X-ray diffraction and crystallography, in a solid to the broadening of a peak in a diffraction pattern, was determined using the Scherrer equation [28]. The pristine HEC based PU sample FPU4 had 2θ=20.016°, reflecting the semi-crystalline nature of the elastomer. The 2θ values of PU bionanocomposite samples FPUNC8, FPUNC9, FPUNC11 and FPUNC13 are 20.207, 19.354, 20.231 and 20.132, respectively (Table 3). The values of 2θ remained intact with increasing %content of TiO_2 nanoparticles. The broadening of the peaks was observed with lower intensity, which can be linked to decrease in crystallinity due to restricted segmental movement by the incorporated TiO_2 nanoparticles in the HEC based PU matrix. It has also been reported that the asymmetric molecular structure of the polyol and diisocyanates used for synthesis of PUs depicts low crystallinity, as seen by the peak intensities [33]. The decrease in intensity of the peaks could also be due to the different chain arrangements formed within the synthesized samples [34]. The results show the nano TiO_2 particles dispersed homogeneously into the HEC based PU matrix, which may prove as a paramount factor for good mechanical properties of the nanocomposites.

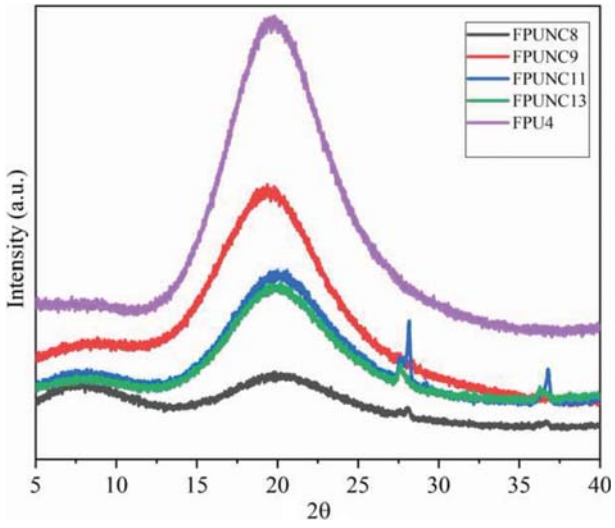

Fig. 4. X-ray diffractograms of pristine HEC based PU elastomer FPU4 and bionanocomposite samples FPUNC8, FPUNC9, FPUNC11 and FPUNC13.

The calculation of the degree of crystallinity (%) and the crystallite size of both neat FPU4 and TiO_2 based bionanocomposites (FPUNC-8, FPUNC-9, FPUNC-11 & FPUNC-13) is shown in Table 3. The % crystallinity and crystallite size values show some variation despite of showing constant affect, by the addition of the TiO_2 content. However, with lower content of TiO_2, the crystallite size decreased a little, which may be related to variation in cooling rate or annealing process. The sample FPU4 without TiO_2 showed semi-crystalline pattern with crystalline size 1.10 and 83% of degree of crystallinity. However, by adding the 1.0% content of TiO_2 in the FPUNC-8 sample, there is a decrease in the degree of crystallinity and the crystalline size, 77% & 0.88, respectively, and the crystallite size again increased with the 2, 4 and 8 wt% content of TiO_2 in the bionanocomposite samples (FPUNC9, FPUNC11 and FPUNC13). The increase in the crystallite size in these samples may be the appearance of sharp peaks at $2\theta \cong 28°$ and $\cong 37°$ corresponding to crystallite size 0.95, 1.12 and 1.15, respectively (Table 3). However, the degree of crystallinity of the samples (FPUNC9, FPUNC11 and FPUNC13) shows some variation with respect to crystallite sizes. The XRD can measure crystalline structure and grain size and both can be calculated directly from XRD data. Note that crystallite size is smaller than the grain or particle size and inside a grain or particle there are many crystals of identical orientation. Furthermore, particle size and grain size are not the same and one particle can have several grains unless someone produces a particle which is a single crystal. Hence, the degree of crystallinity may not purely relate to the crystallite size.

3. Scanning Electron Microscope (SEM) Analysis

The SEM techniques provide a unique way to visualize the morphology of the nanocomposites. The SEM images of PU nanocomposites with 0.5% TiO_2 nanoparticles (FPUNC8), with 2.0% TiO_2 nanoparticles (FPUNC9) and with 4.0% TiO_2 nanoparticles (FPUNC11) are presented in Fig. 5(a), (b), and (c). Although TiO_2 nanoparticles tend to strongly agglomerate, causing poor dispersio within a PU matrix, however in the current study, the images reveal the uniform distribution of TiO_2 nanoparticles embedded in the polymer matrix with uniform surfaces due to their strong intermolecular forces caused by increased area. No visible cracks were observed. An enhanced level of exfoliation was observed with the increase in %wt of the nanoparticles thoroughly dispersed in the polymer matrix. Due to their strong intermolecular forces, the TiO_2 nanoparticles seem to be directly attached with the polymeric chains, showing a uniform distribution, which in turn is very helpful for improvement of thermal and mechanical properties of

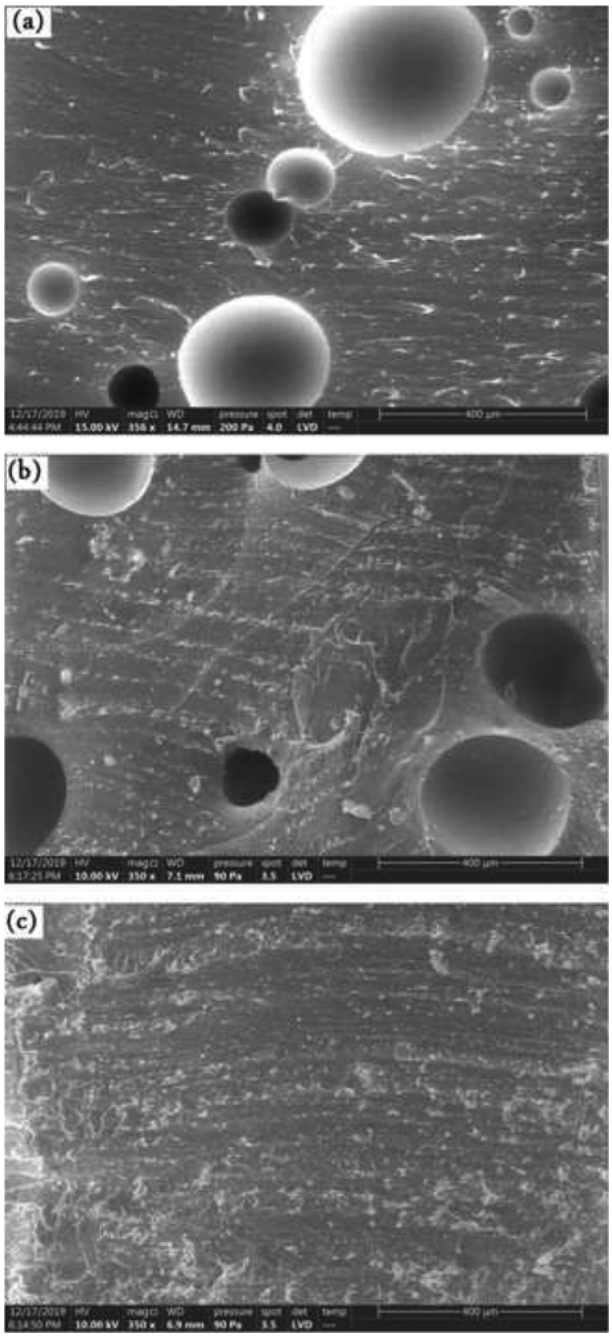

Fig. 5. Scanning electron microscope (SEM) images of (a) FPUNC7; (b) FPUNC9; (c) FPUNC13 (with 400 nm scale marker for all three images (a), (b) and (c)).

the bionanocomposites. The nanoparticles are easily recognizable in the presented images. Alam et al. reported such regular or even dispersion of the nano materials as an essential condition to avoid structural defects in the nanocomposite materials [1]. It is pertinent to mention here that rutile TiO_2 nanoparticles have high UV opacity and low photoactivity, and are effective UV protectors for several polymer systems including PU. On the basis of its outstanding opacity, the material can be effectively used as excellent UV protective in combination with PU having better outdoor exposure resistivity.

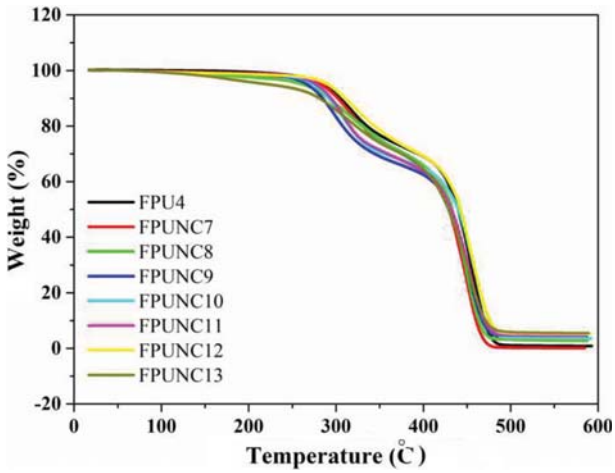

Fig. 6. TGA curves of HEC based PU elastomer FPU4 and TiO_2 nanoparticle based HEC-PU bionanocomposites FPUNC7-FPUNC13.

4. Thermo-gravimetric (TG) Analysis

In Fig. 6 TG curves of pristine HEC based polyurethane elastomer (FPU4) and TiO_2 nanoparticles based HEC-PU bionanocomposites (FPUNC7-FPUNC13) are presented. Thermogravimetric analysis (TGA) has been reported to be a handy tool for the thermal stability of the synthesized PUs [35]. The thermal stability (20% and 80% wt loss) data of the HEC based PU bionanocomposites with TiO_2 is presented in Table 2. Conventionally, the TG curves indicated the weight loss in the prepared bionanocomposites in two prominent stages. A minor change in weight loss occurred between 200-300 °C, and major loss in weight was observed between 300-470 °C, which reveals that the material can be used for potential industrial application where working condition is up to 200 °C . As there is no -OH peak in the FTIR spectra of final PU, so the change in weight loss in the range of 200-300 °C is not related to loss of some unreacted small molecules (1,4-butanediol, boiling point=230 °C or other) directing to the fact that there is complete reaction. The combination of organic-inorganic materials at the exterior of nanocomposite influences their thermal stability. The hydroxyethyl cellulose possesses good chemical affinity with polyurethane. The reduced particle size of nanomaterial also provides a greater surface area to form stable complexes within the bio composites, making them thermally more stable [36,37]. Consequently, the synthesized bionanocomposite exhibits comparable stability relative to its components under diverse environmental conditions [38]. The TGA results of the PU bionanocomposites shows the onset degradation temperature (T_{onset}) is almost the same as the control PU even after increasing TiO_2 wt% in PU samples, which indicates that the desorption or drying in the studied samples occurs in the same pattern. In addition, there is not much change in T-80% of TiO_2 containing samples as compared to control PU which implies that mass loss of all the samples is large and similar followed by mass plateau. These results are in accord with previous findings [39]. Of note is that TGA curves are dependent on absolute temperature and time spent at that temperature; any

Table 3. Crystallite size and degree of crystallinity and of different formations of TiO_2 based polyurethane bionanocomposites

Sample code	TiO_2 wt (%)	2 theta (θ)	FWHM[a]	Crystallite size	d-Spacing	Degree of crystallinity (%)[b]
FPU4	0.0	20.016	7.436	1.10	0.013	83±0.31
FPUNC8	1.0	20.207	9.327	0.88	0.013	77±0.22
FPUNC9	2.0	19.354	8.597	0.95	0.012	87±0.42
FPUNC11	4.0	20.231	7.347	1.12	0.013	65±0.36
FPUNC13	8.0	20.132	7.149	1.15	0.013	69±0.27

[a]The full width at half maximum (*FWHM*) of *XRD* profiles.
[b]Calculated multiplying the ratio of the crystalline peak area to total peak area by 100.

experimental parameter that can affect the reaction rate will change the shape/transition temperatures of the curve, so the similar behavior of the samples and the control has been recoded as the content of TiO_2 has been varied keeping other monomer ratio remaining the same. The results revealed that the sample with 5 wt% TiO_2 (FPUNC12) shows better thermal stability and it provides slightly higher T-20% than the control PU sample, while all other TiO_2 containing samples have rather lower T-20% temperature than the control PU sample. Such thermal pattern might be due to optimized concentration of TiO_2 with better dispersibility. The HEC based polyurethane bionanocomposites having TiO_2 nanoparticles are good candidates for their application in the temperature range of up to 200 °C and good biological applications.

CONCLUSION

The combination of hydroxyethyl cellulose (HEC) and TiO_2 nanoparticles has been successfully utilized for the preparation of novel environment-friendly polyurethane bionanocomposites. The HEC based PUs prepolymers blended with TiO_2 nanoparticles were synthesized to get final polyurethane bio-nanocomposites. The structural elucidation of the synthesized PU bionanocomposites was confirmed by FTIR. Their morphological and thermal properties were studied with the help of XRD, SEM and TGA techniques. The homogeneous dispersion of TiO_2 nanoparticles into PU matrix was verified by SEM images. The results revealed that the sample FPUNC12 with 5% content of TiO_2 nanoparticles showed better thermal stability. The results depicted homogeneous exfoliation of the nanoparticles in the bionanocomposite pivot role in enhancing its thermal properties. The results revealed that with the increase in TiO_2 nanoparticles in the FPUBNC formulation, the 2θ value increased and resultantly the broadening of the peaks was also observed with lower intensities, which can be linked to strong interfacial interactions among the TiO_2 nanoparticles and the HEC based PU matrix. It can be concluded that HEC based polyurethane bionanocomposites having TiO_2 nanoparticles are bio-degradable, bio-functional materials with good thermal properties and have potential applications in the field of biomaterials.

REFERENCES

1. K. Mahmood, K. M. Zia, M. Zuber, Zill-i-Huma Nazli, S. Rehman and F. Zia, *Korean J. Chem. Eng.*, **33**, 3316 (2016).
2. F. Mumtaz, M. Zuber, K. M. Zia, T. Jamil and R. Hussain, *Korean J. Chem. Eng.*, **30**, 2259 (2013).
3. M. Alizadeh-Sani, A. Khezerlou and A. Ehsani, *Ind. Crops Prod.*, **124**, 300 (2018).
4. A. Noreen, K. M. Zia, M. Zuber, S. Tabasum and M. J. Saif, *Korean J. Chem. Eng.*, **33**, 388 (2016).
5. Y. Zhang, Q. Jin, J. Zhao, C. Wu, Q. Fan and Q. Wu, *Eur. Polym. J.*, **46**, 1425 (2010).
6. S. K. Dogan, S. Boyacioglu, M. Kodal, O. Gokce and G. Ozkoc, *J. Mech. Behav., Biomed. Mater.*, **71**, 349 (2017).
7. A. Simmons, J. Hyvarinen and L. Poole-Warren, *Biomaterials*, **27**, 4484 (2006).
8. O. V. Alekseeva, A. N. Rodionova, N. A. Bagrovskaya, A. V. Agafonov and A. V. Noskov, *Cellulose*, **24**, 1825 (2017).
9. M. A. Hubbe, O. J. Rojas and L. A. Lucia, *BioResources*, **10**, 6095 (2015).
10. L. Satish, K. Achary, A. Kumar, B. Barik, P. S. Nayak, N. Tripathy, J. P. Kar and P. Dasha, *Sensor. Actuat. B-Chem.*, **272**, 100 (2018).
11. K. Gorna, S. Polowinski and S. Gogolewski, *J. Polym. Sci. Part A Polym. Chem.*, **40**, 156 (2002).
12. K. M. Zia, M. Zuber, I. A. Bhatti, M. Barikani and M. A. Sheikh, *Int. J. Biol. Macromol.*, **44**, 23 (2009).
13. F. Zia, K. M. Zia, Z. i. H. Nazli, S. Tabasum, M. K. Khosa and M. Zuber, *Int. J. Biol. Macromol.*, **153**, 591 (2020).
14. K. M. Zia, M. Zuber, M. J. Saif, M. Jawaid, K. Mahmood, M. Shahid, M. N. Anjum and M. N. Ahmad. *Int. J. Biol. Macromol.*, **62**, 670 (2013).
15. K. Benhamou, H. Kaddami, A. Magnin, A. Dufresne and A. Ahmad, *Carbohydr. Polym.*, **122**, 202 (2015).
16. M. A. Hubbe, D. J. Gardner and W. Shen, *BioResources*, **10**, 8657 (2015).
17. K. M. Zia, K. Mahmood, M. Zuber, T. Jamil and M. Shafiq, *Int. J. Biol. Macromol.*, **59**, 320 (2013).
18. M. Zuber, K. M. Zia, S. Mahboob, M. Hassan and I. A. Bhatti, *Int. J. Biol. Macromol.*, **47**, 196 (2010).
19. K. Mahmood, K. M. Zia, M. Zuber, M. Salman and M. N. Anjum, *Int. J. Biol. Macromol.*, **81**, 877 (2015).
20. A. M. Youssef, S. M. El-Sayed, H. H. Salama, H. S. El-Sayed and A. Dufresne. C*arbohyd. Polym.*, **132**, 274 (2015).
21. M. H. A. Rehim, A. M. Youssef and A. Ghanem, *Polym. Bull.*, **72**, 2353 (2015).
22. A. M. Youssef, F. M. Malhat and A. F. A. Abd El-Hakim, *Polym. Plast. Technol. Eng.*, **52**, 228 (2013).
23. A. M. Youssef, *RSC Adv.*, **4**, 6811 (2014).
24. A. A. Hebeish, M. M. Abdelhady and A. M. Youssef, *Carbohydr.*

Polym., **91**, 549 (2013).
25. X. Kong, L. Zhao and J. M. Curtis, *Carbohydr. Polym*., **152**, 487 (2016).
26. K. M. Zia, M. Zuber, M. Barikani, A. Jabbar and M. K. Khosa, *Carbohydr. Polym*., **80**, 539 (2010).
27. M. Fiayyaz, K. M. Zia, M. Zuber, T. Jamil, M. K. Khosa and M. A. Jamal, *Korean J. Chem. Eng*., **31**, 644 (2014).
28. A. Patterson, *Phys. Rev*., **56**, 978 (1939).
29. A. Noreen, K. M. Zia, S. Tabasum, W. Aftab, M. Shahid and M. Zuber, *Int. J. Biol. Macromol*., **151**, 993 (2020).
30. K. Mahmood, K. M. Zia, M. Zuber, S. Tabasum, S. Rehman, F. Zia and A. Noreen, *Int. J. Biol. Macromol*., **105**, 1180 (2017).
31. N. Sun, T. Wang and X. Yan, *Carbohydr. Polym*., **172**, 49 (2017).
32. I. Fleming and D. Williams, *Spectroscopic methods in organic chemistry*, 7th Ed., Springer International Publishing, Springer Nature Switzerland AG (2019).
33. W. Han, M. Tu, R. Zeng, J. Zhao and C. Zhou, *Carbohydr. Polym*., **90**, 1353 (2012).
34. S. Taheri and G. M. M. Sadeghi, *Appl. Clay Sci*., **114**, 430 (2015).
35. I. Javni, Z. S. Petrović, A. Guo and R. Fuller, *J. Appl. Polym. Sci*., **77**, 1723 (2000).
36. P. Coimbra, P. Alves, T. A. M. Valente, R. Santos, I. J. Correia and P. Ferreira, *Int. J. Biol. Macromol*., **49**, 573 (2011).
37. W. Wang, T.-J. Zhang, D.-W. Zhang, H.-Y. Li, Y.-R. Ma, L.-M. Qi, Y.-L. Zhou and X.-X. Zhang, *Talanta*, **84**, 71 (2011).
38. M. Safaei and M. Taran, *Int. J. Biol. Macromol*., **104**, 449 (2017).
39. S. Loganathan, R. B. Valapa, R. K. Mishra, G. Pugazhenthi and S. Thomas, in *Thermogravimetric analysis for characterization of nanomaterials at in micro and nano technologies, thermal and rheological measurement techniques for nanomaterials characterization*, S. Thomas, R. Thomas, A. K. Zachariah, R. K. Mishra Eds., Elsevier, Amsterdam (2017).